Robert Mark*, Nipun Mishra, Kaushik Mandal, Partha Pratim Sarkar and Soma Das

Hexagonal Nested Loop Fractal Antenna for Quad Band Wireless Applications

https://doi.org/10.1515/freq-2018-0115
Received May 14, 2018

Abstract: A compact hexagonal nested loop fractal antenna with L shaped slot on the ground plane is presented for multiband applications. In this paper, the effect of fractal iterations and position of L-slot on ground plane are optimized for better performance of the antenna. Multiple hexagon loops excite multiple resonant modes at 1.7, 2.4, 3.1, 4.5 and 6 GHz and an L-shaped slot on the ground plane helps to achieve wide bandwidth response with better impedance matching in the 4.25–6.41 GHz frequency band. An equivalent circuit of the proposed antenna is modelled and the same is verified using ADS. Reflection coefficient and radiation pattern are presented to further confirm the performance of the proposed design for wireless applications. The proposed antenna is fabricated on a low-cost FR4 substrate of dimensions $40 \times 32 \times 1.6$ mm^3 and measured results show good agreement with simulation results.

Keywords: hexagonal nested loop, fractal, iteration, multiband, microstrip antenna

1 Introduction

In recent years, extensive development in wireless application demands antenna to be more compact to integrate multiple wireless standards with wideband characteristics to support high data rate applications. The multiband antenna is therefore becoming more and more favourable with the advancement of technology which inherently includes design challenges like small-size, ease of fabrication, low cost, high performance and wide bandwidth. This profound demand for new design concepts introduces various compact and multiband techniques like CPW feed monopole [1, 2], self-similar ring radiators [3], and monopole with defected ground plane [4–6]. However, fractals which have self-similarity and self-affinity in their structures can offer miniaturization with multiband characteristics [7] and can prove them a better candidate for designing a compact multiband antenna. Various planar curve fractals for multiband using Koch, Sierpinski, Minkowski, and Hilbert have been implemented in design [8–10]. Several CPW fed fractal antennas with slot are reported for broadband covering WLAN and WiMAX band with design space minimization [11, 12]. Self-affine cantor multi fractals also provide flexibility in controlling the resonance over larger design space [13, 14]. Geometry like E-shaped fractal antenna [15] designed with an air gap between substrate and ground plane is proposed for multiband application whereas H shape, X shape and Pythagoras tree fractal [16–18] utilizing self-similar repeating structures are reported but most of them have a large size and complicated structure. The elliptical ring monopole antenna with conductor backed plane [19] is also proposed for multiband but with moderate gain over the desired frequency band. The Triband operation covering GSM/WLAN/WiMAX band are discussed in [20, 21] using the various crinkle shaped curve and spiral rings fractals. In comparison to conventional curves and alphabet based fractal geometries, the miniaturization of antenna dimensions is shown to be effective and compact by taking nested loop geometries as discussed in more recent designs [19–21].

In this paper, we have reported a hexagonal nested loop fractal antenna with L- shaped slot on the ground plane for quad-band frequency operation. Numbers of operating bands are related with the numbers of nested loops. Impedance matching and bandwidth of the operating bands are influenced by the position of the slot on the ground plane. The proposed antenna was fabricated and measured. Details of antenna design steps, parametric studies, and experimental results like $|S_{11}|$ curves, radiation patterns, and current distribution are discussed and explained.

2 Antenna design

The proposed antenna has been designed with 50-Ω asymmetric microstrip line feed printed on FR4 substrate

***Corresponding author: Robert Mark,** Department of ECE, Guru Ghasidas Vishwavidyalaya, (Central University), Bilaspur, India, E-mail: mark.robert.1989@ieee.org
http://orcid.org/0000-0003-4363-8859
Nipun Mishra, Department of ECE, Guru Ghasidas Vishwavidyalaya, (Central University), Bilaspur, India
Kaushik Mandal, Institute of Radio Physics and Electronics, University of Calcutta, Calcutta, India
Partha Pratim Sarkar, DETS, University of Kalyani, Kalyani, India
Soma Das, Department of ECE, Guru Ghasidas Vishwavidyalaya, (Central University), Bilaspur, India

($\in_r$ = 4.4) of height 1.6 mm, loss tangent tan δ = 0.025 and area 32 (x axis) x 40 (y axis) mm^2. The hexagon nested loop fractal antenna with a partial ground plane of dimension (L_g x W = 9.8 mm x 32 mm) printed on the bottom side of the patch as shown in Figure (1). The width of hexagon ring strip optimized to W_s = 1 mm and remain constant for all consecutive rings in the entire process of simulation and observation. The gaps L_1-L_3 are obtained respectively corresponding to the calculation of the sides of hexagon using eq. (1). The optimized dimensions of antenna were obtained by performing parametric analysis on antenna dimensions L_4, L_5, L_g, W_f and g for better impedance matching in the desired frequency bands. Antenna bandwidth has been further enhanced with an L-shaped slot on the ground plane as shown in Figure (1b). Sides of the regular hexagon at various stages are related to scaling factor and can be determined by following equation [17]:

$$S_{n+1} = \theta.S_n \quad (1)$$

Where n (= number of Iteration) = 1, 2, 3; S_1 is initial length of hexagon side (Initiator)

The scale factor, Θ is the factor whose value lies between 0 and 1. Initiator geometry is multiplied with scale factor, which is the controlling parameter in designing the proposed antenna for desired multiband operation. For this design the scale factor is optimized to Θ = 0.734. To achieve other desired frequency band, we have to first design the initiator at some standard desired operating cut off frequency and then by using a proper scaling factor, we can achieve the lower desired frequency bands. The final design also requires some more parametric optimization to obtain exact desired frequency bands. The evolution of the proposed antenna structure from initiator geometry of single ring hexagon to the final design with L shaped slot is shown in Figure (2). Antenna with initiator ring resonates at three frequencies which are shifted towards lower frequency side by the addition of second ring (first fractal). By nesting hexagon ring to the initiator geometry the number of resonance frequency increases. The number of hexagon ring is consecutively added in the design to achieve proper multiband operation. Figure 3 shows the comparison result of the simulated S_{11} parameter for various iteration stages and finally with the proposed antenna. The computer simulation technology software (CST) has been used to optimize the performance of the antenna. The final dimensions of the proposed antenna are summarized in Table 1.

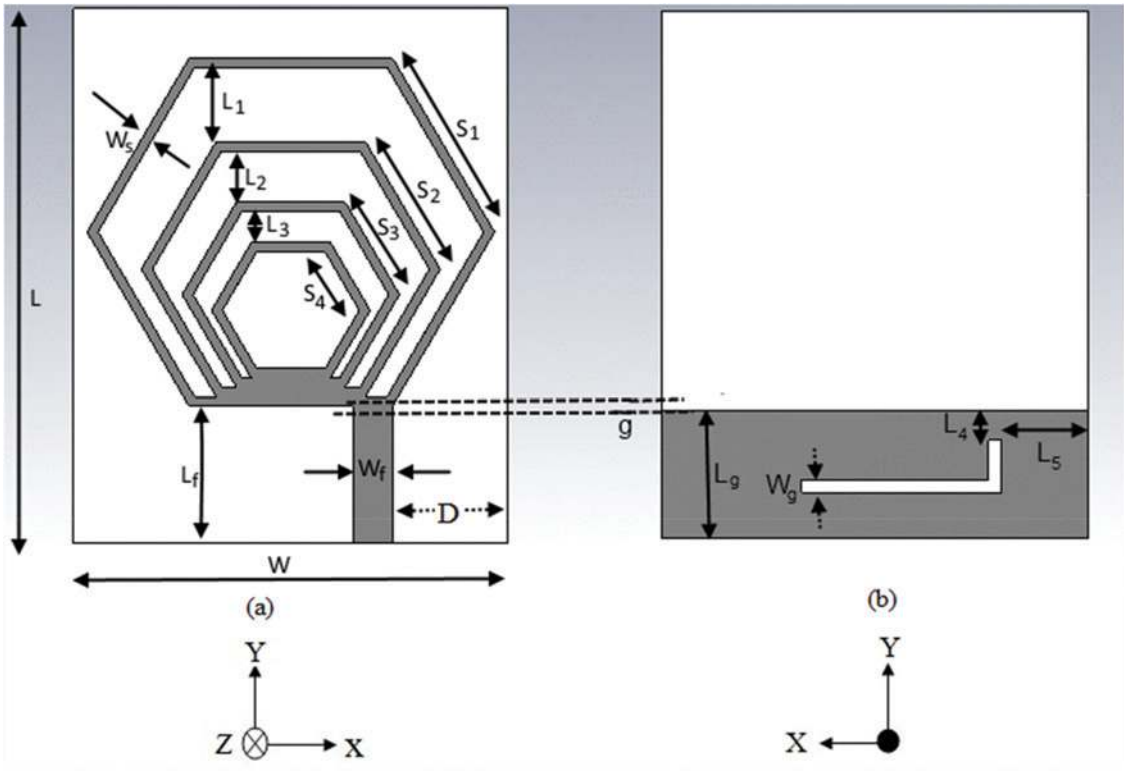

Figure 1: Proposed antenna (a) front view (b) back view.

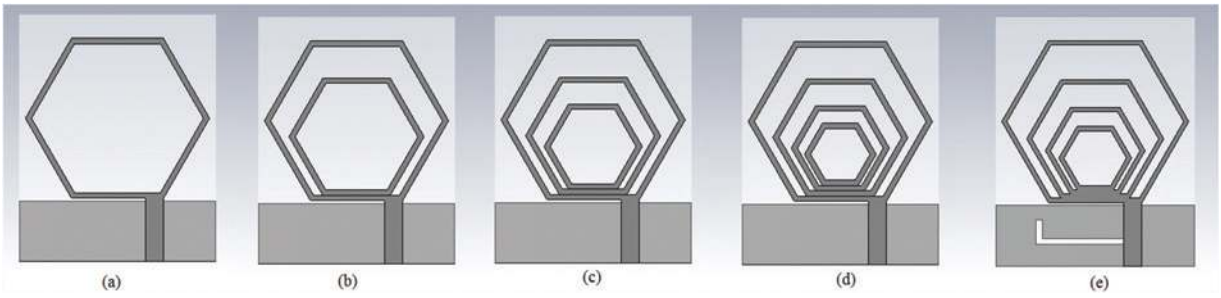

Figure 2: Design steps of proposed antenna (a) Initiator (b) First Fractal (c) Second Fractal (d) Third fractal (e) Proposed design.

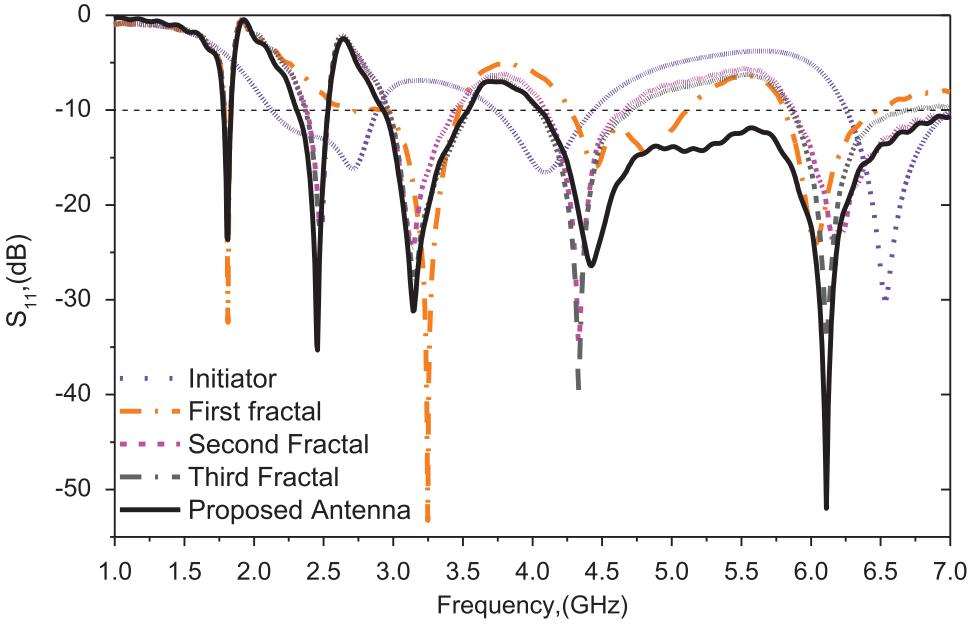

Figure 3: Simulated S_{11} of antenna for various design steps as shown in Figure 2 (a)-(e)..

Table 1: Dimensions of proposed antenna.

Parameter	Dimension (mm)	Parameter	Dimension (mm)
L	40	S_1	15
L_g	9.8	S_2	11
L_f	10.3	S_3	8.0
L_1	5.2	S_4	5.9
L_2	3.5	W	32
L_3	2	W_S	1
L_4	2	W_f	2.9
L_5	6	W_g	1
g	0.5	D	8.6

1 Effect of slot position (L_5 &L_4)

The dimension of slot on ground plane can be determined by:

$$f_L = \frac{c}{4 \times L_{Slot}} \tag{2}$$

Where, c is the speed of light, f_L is the lower cut off frequency of wideband (4.25–6.41 GHz), L_{slot} is the length of the slot on the ground plane. Thus the length of the slot in the proposed design approximately obtained at 18 mm. Parametric analysis has been done for proper positioning of the slot on the ground plane to achieve

wide impedance bandwidth and better impedance matching. It is observed that as the position of L shaped slot moves toward feed line from point A (L_5 = 0) to L_5 = 10 in Figure 1(b), the resonances at 4.5 and 6 GHz band merge to form wideband response and the impedance bandwidth also increases as shown in Figure 4(a). The position of the slot from top of the ground plane, L_4 controls the impedance bandwidth. As slot moves from the top of

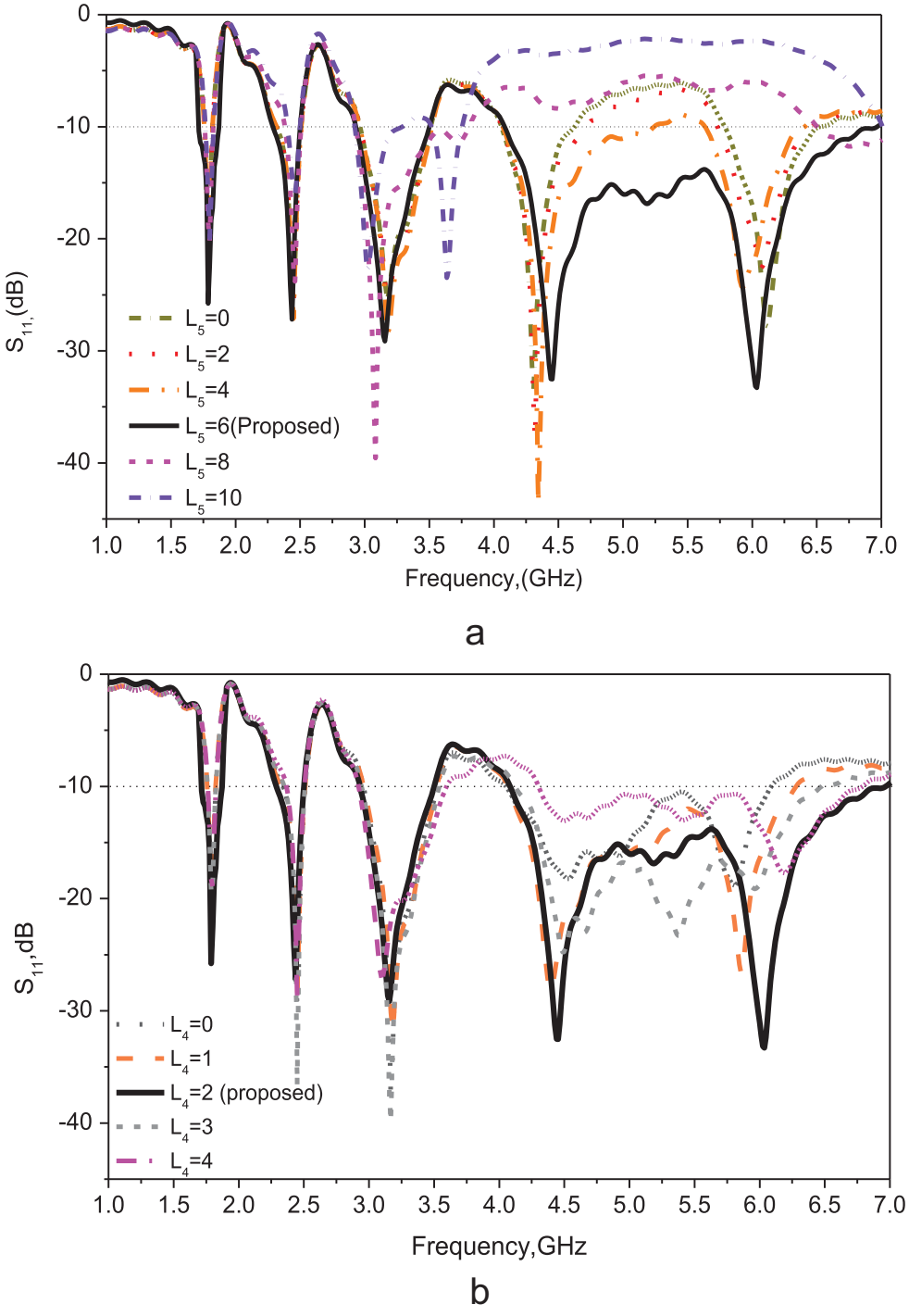

Figure 4: (a) Effect of slot position along x-axis (horizontal movement) with respect to different value of L_5 on ground plane for L_4 = 2 mm (constant) as shown in Figure 1(b). (b) Effect of slot position along y axis (vertical movement) with respect to different value of L_4 on ground plane for L_5 = 6 mm (constant) as shown in Figure 1(b).

the ground plane towards L_4 = 6 mm, the bandwidth increases and becomes maximum for L_4 = 2 mm and then decreases as it moves closer to SMA feed point shown in Figure 4(b). From the parametric analysis of the slot on both x and y axis on the ground plane, the position of the slot is fixed at L_5 = 6 mm and L_4 = 2 mm for best performance of antenna with an impedance bandwidth of 2.16 GHz (6.41–4.25 GHz). This result establishes that as the slot moves closer to the feed line, impedance matching improves due to better coupling. From simulation results, we conclude that with the increase of iteration stages, the antenna dimension decreases in Y-direction causing total electrical path length to increase, that shifts the resonant frequency towards lower frequency side and provides multiple resonances [13–19].

3 Results and discussion

The proposed antenna in the earlier section has been fabricated as shown in Figure 5. The measurement of the fabricated antenna is performed using an Agilent N9926A vector network analyzer. The measured and simulated S_{11} parameters of the antenna are shown in Figure 6, with little discrepancies due to fabrication tolerances of the antenna that may lead to the shift of resonating frequency from 3.1 GHz to 3.5 GHz. The shifting in resonance frequency may also be due to the cable loss during the measurement of antenna by VNA and it is within the acceptable limit. It can be seen that the antenna operates in four frequency band with resonating frequency at 1.7, 2.4, 3.1, 4.5 and 6 GHz and measured impedance bandwidth (S_{11} < −10 dB) of 10.7 % (1.88–1.69 GHz), 7.5 % (2.52–2.34 GHz), 15.2 % (3.57–3.07 GHz) and 40 % (6.41–4.25 GHz) respectively, which meet the bandwidth requirement of DCS or GSM1800, LTE2300, Bluetooth and WLAN 5.2/5.8 GHz, WiMAX band at 3.5 GHz frequency.

The simulated real and imaginary impedance of the proposed antenna are shown in Figure 7 with better impedance matching over the operating frequency band and it is observed that near the resonant frequencies, the real impedance approaches close to 50 Ω. In order to understand physical behaviour of multiband antenna, surface current distributions over the design surface are compared in Figure 8. It can be derived from the comparative study of Figure 8(a) and 8(b) that current is concentrated near the outer edge of initiator and second ring at 1.7 and 2.4 GHz respectively, which indicates that larger outer ring provides the electrical current path for 1.7 GHz and inner ring responsible for 2.4 GHz resonance. It can be seen from Figure 8(c) current density is maximum in the alternate sides of the outer patch as well as along the edges of the third ring which shows that addition of the third ring contributes the 3.1 GHz resonance. However, at 4.5 GHz and 6 GHz frequencies, current is mainly concentrated near the edges of L-shaped slot on the ground plane signifying that the length of the current path depends on position and length of the slot coupled to feed line which in turn causes additional bandwidth enhancement and also validates the effects of slot in the given band of operation.

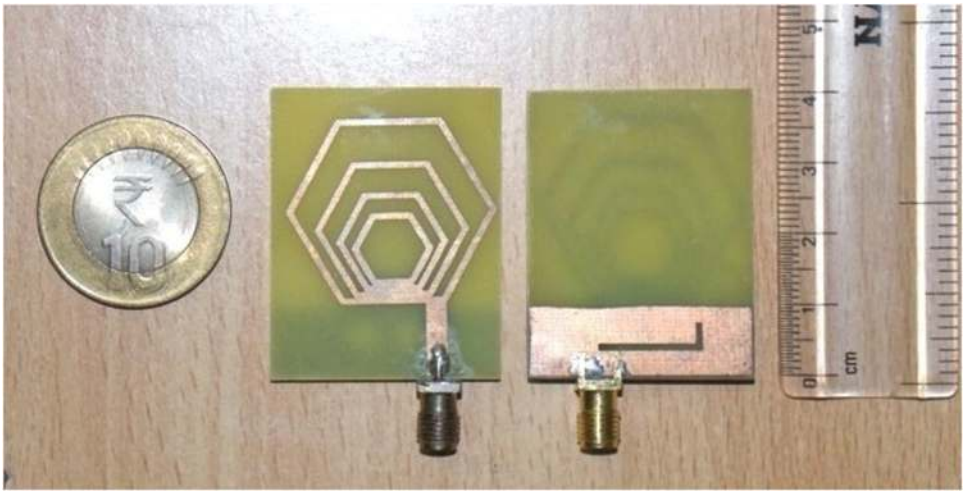

Figure 5: Photograph of the fabricated antenna.

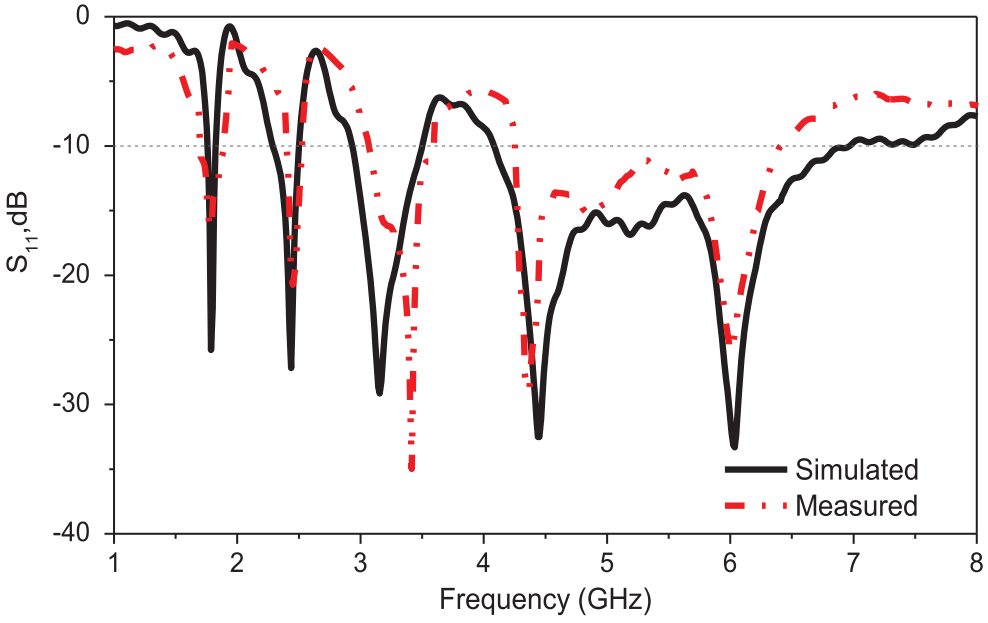

Figure 6: Measured and Simulated S_{11} for proposed design antenna at 1.7 GHz, 2.4 GHz, 3.1 GHz, 4.5 GHz and 6.0 GHz.

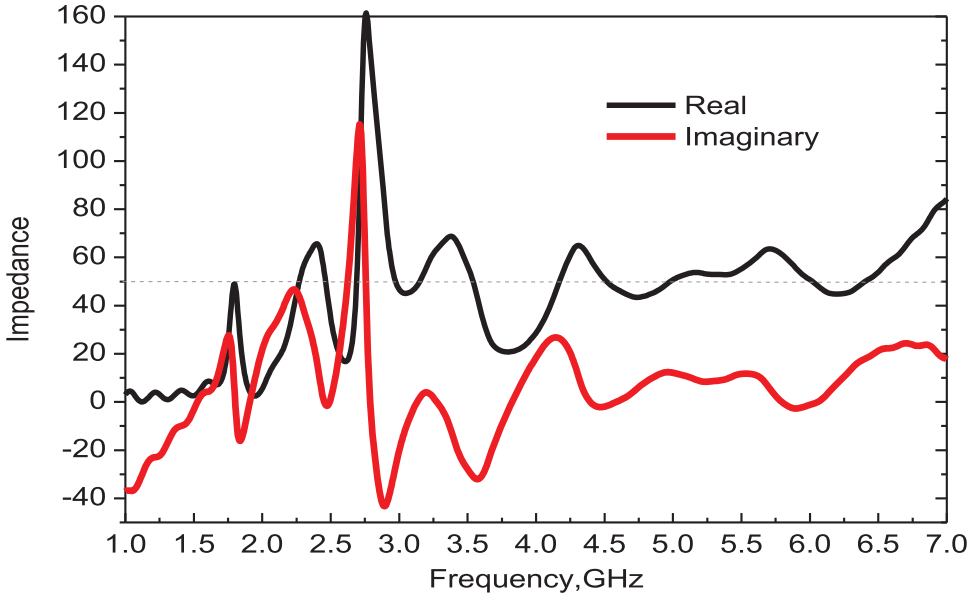

Figure 7: Simulated real and imaginary impedance of the proposed antenna.

Measured far field radiation patterns of the proposed antenna are shown in Figure 9 (Co & Cross Polarization) at 1.7 GHz, 2.4 GHz, 3.1 GHz and 5.4 GHz (center frequency of 6.41–4.25 GHz band). The proposed antenna shows omni directional characteristics in H-plane and has a bidirectional pattern in E-plane with small cross polarization level.

Figure 10 shows the measured gain of the proposed antenna and is determined as 1.6, 2.15, 2.79 and 3.8 dBi for 1.7, 2.4, 3.1 and 5.4 GHz with simulated radiation efficiency of 64 %, 91 %, 87 % and 67 % at 1.7, 2.4, 3.1 and 5.4 GHz frequency respectively. Table2 shows the comparison result of our proposed work with reported literature in terms of operating bandwidth, dimension,

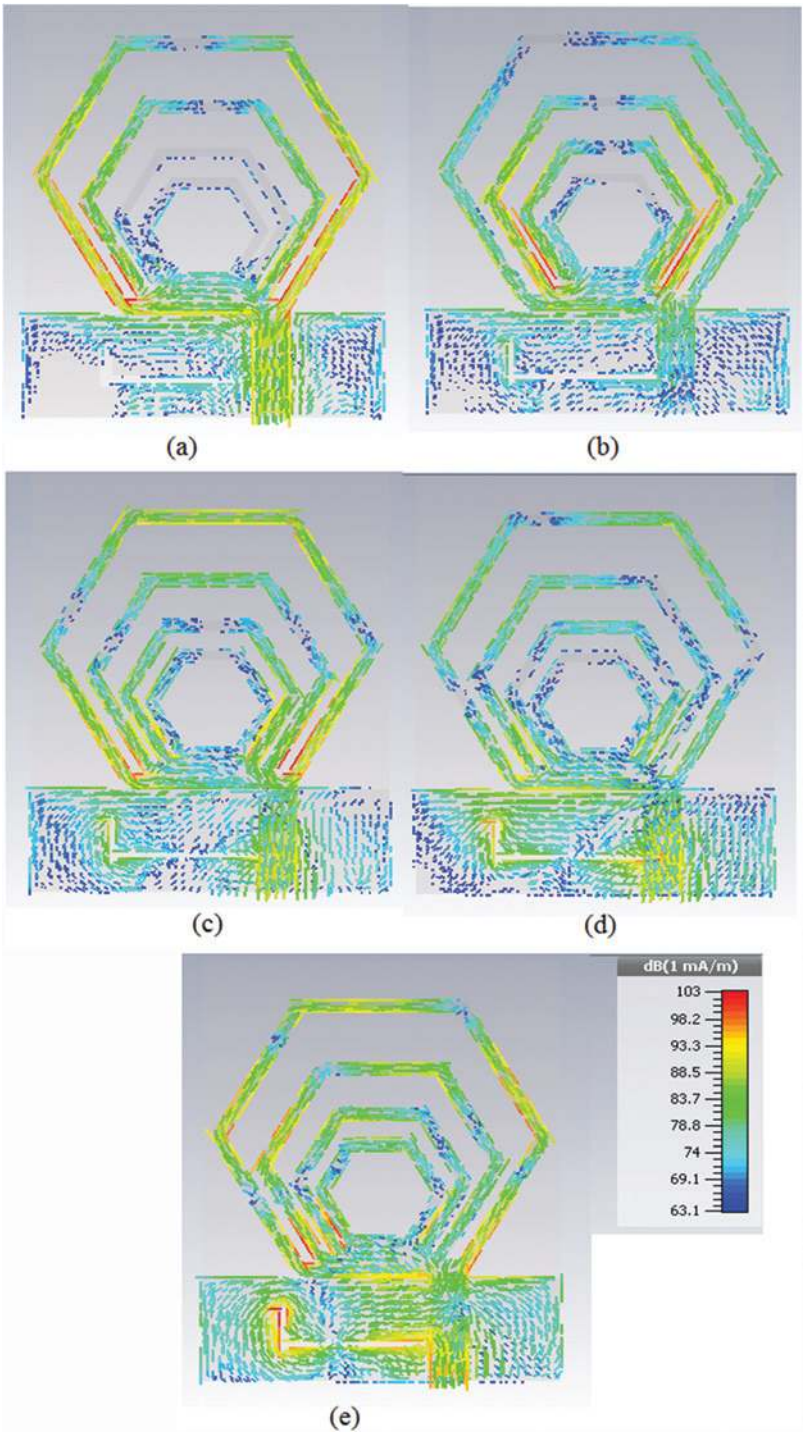

Figure 8: Simulated surface current distributions on the radiating patch of proposed antenna at (a) 1.7 GHz (b) 2.4 GHz (c) 3.1 GHz (d) 4.5 GHz (e) 6 GHz.

gain, efficiency and application covered. The comparison shows that the proposed design offer quad-band frequency operation with design dimension compact and suitable for portable wireless devices.

4 Conclusion

Hexagonal nested loop fractal antenna of size $40 \times 32 \times 1.6\,mm^3$ with L-shaped slot has been designed and

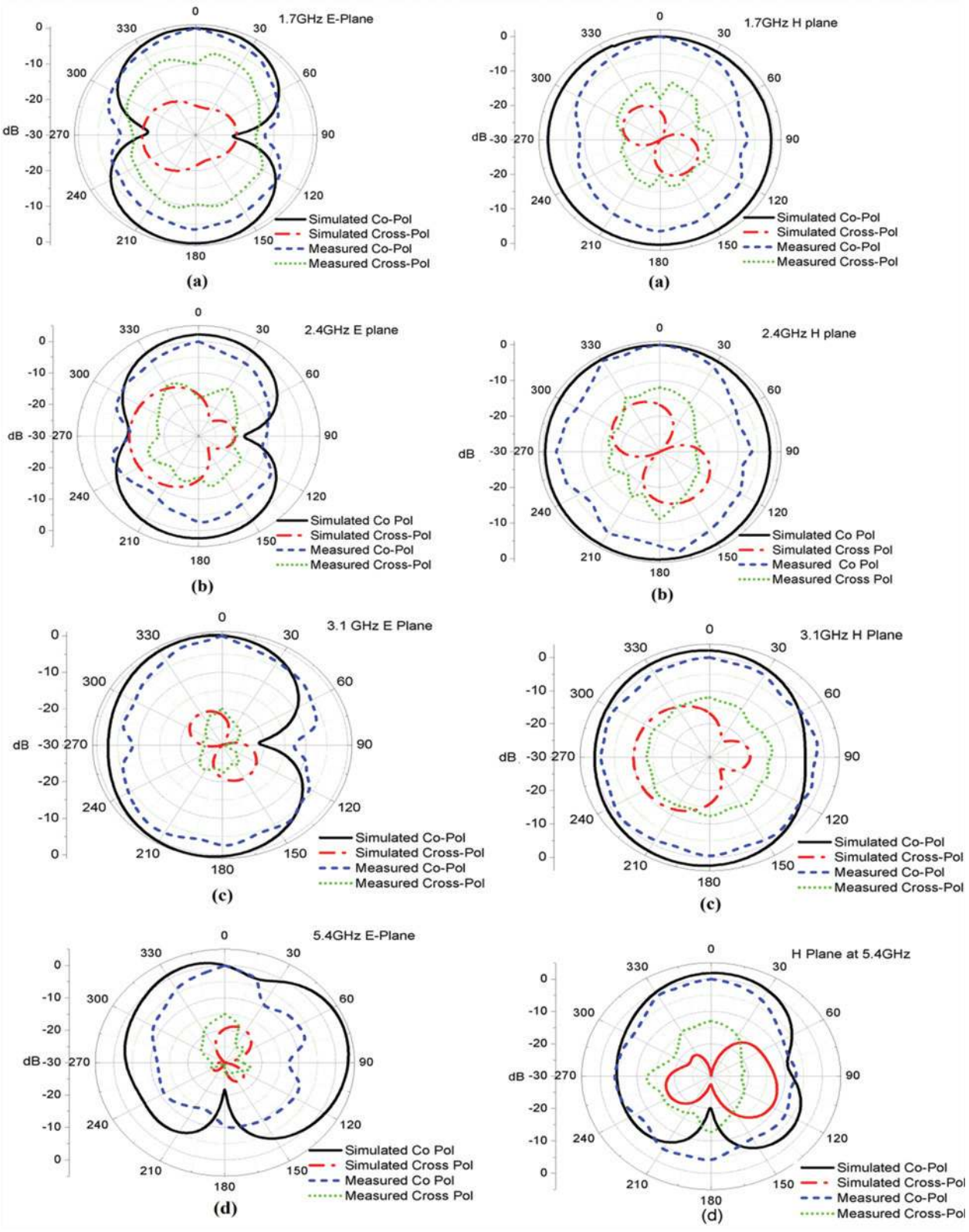

Figure 9: Simulated and Measured Co and Cross Pol of proposed antenna in E(yz plane) and H (xz-plane) planes at (a) 1.7 GHz (b) 2.4 GHz (c) 3.1 GHz (d) 5.4 GHz.

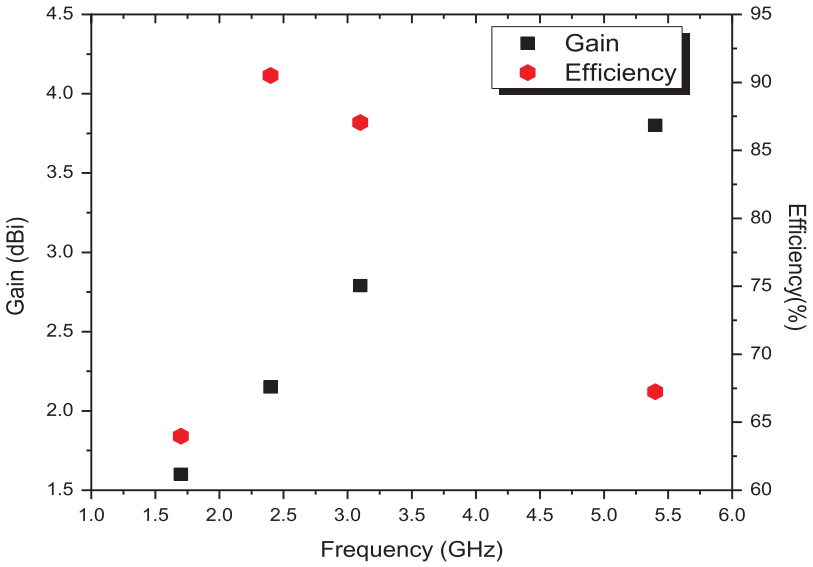

Figure 10: Measured Gain and Simulated Efficiency of proposed antenna.

Table 2: Comparison between the proposed antenna and other antennas.

S. No	Ref.	Size (mm^2)	Resonating Frequency (GHz)	Operating Band (GHz)	Gain (dBi)	Efficiency (%)	Number of Bands	Application Covered
1	[3]	25 x 38	2.5, 3.5,5.8	(2.35–2.8), (3.4–3.7), (5.05–6.1)	2.36, 2.75, 3.62	... .	Triple band	WLAN, WiMAX
3	[4]	30 x 40	0.94, 2.7,4.75	(912–972), (2.39–3.943), (4.689–5.324)	–3.67, 1.34, 4.94	55, 72, 82	Triple band	GSM 900,WLAN
2	[6]	34 x 18	2.5,3.5,5.5	(2.41–2.70, 3.32–3.72, (5.39–5.74)	0.28, 1.42, 4.76	86.3, 87.6, 85.9	Triple Band	WLAN, WiMAX
4	[17]	120 x 87	0.36, 1.32, 5.50	(2.4–2.497),(5.15–5.825)	1.91, 3.72, 7.52	–	Dual band	2.45/5.5-GHz WLAN
6	[18]	88 x 108	2, 3.5, 4.9, 6.5	(1.980–2.010), (3.40–3.50), (4.94–4.99),(6.0–6.8)	3.23,4.3,5.954.65	46, 79, 73,58	Quad Band	WMAN,WLAN
5	[21]	14 x 14	1.780,3.520,5.2	(1.691–1.880), (3.412–3.624), (5.139–5.441)	Peak Gain 2.7	–	Triple Band	GSM1800, WiMAX, WLAN
7	**This Work**	32 x 40	1.7, 2.4, 3.1, 4.5, 6	(1.69–1.88), (2.34–2.52), (3.07–3.57), (4.25–6.41)	1.6, 2.15, 2.79,3.8	64, 91, 87, 67	Quad Band	GSM1800,2.4/ 5.2/5.5 WLAN, WiMAX

fabricated on FR-4 substrate for DCS or GSM1800, LTE2300, Bluetooth and WLAN 2.4/5.2/5.8 GHz, WiMAX band of operation. Numbers of hexagon loop rings are optimized to obtain different resonant modes with excellent impedance bandwidth performance. Variation of the L-shaped slot parameters and its positions on the ground plane are studied in details to achieve a wide bandwidth. The fabricated antenna offers quad-band frequency response with stable far-field radiation patterns and reasonable gain. A comparison with the available design from the literature shows that the proposed design offers quad band frequency operation with design dimension compact and suitable for portable wireless devices.

References

[1] R. Ghatak, R. K. Mishra, and D. R. Poddar, "Perturbed Sierpinski Carpet Antenna with CPW Feed for IEEE 802.11 a/b WLAN Application," *IEEE Antennas Wirel. Propag. Lett.*, vol. 7, pp. 742–744, 2008.

[2] G. Augustin, P. C. Bybi, V. P. Sarin, P. Mohanan, C. K. Aanandan, and K. Vasudevan, "A compact dual-band planar antenna for DCS-1900/PCS/PHS, WCDMA/IMT-2000, and WLAN applications," *IEEE Antennas Wirel. Propag. Lett.*, vol. 7, pp. 108–111, 2008.

[3] W. X. Liu, Y. Z. Yin, and W. L. Xu, "Compact self similar triple band antenna for WLAN/WiMAX applications," *Microw. Opt. Technol. Lett.*, vol. 54, no. 4, pp. 1084–1087, Apr. 2012.

[4] H. F. Abutarboush, H. Nasif, R. Nilavalan, and W. Cheung, "Multiband and Wideband Monopole Antenna for GSM900 and Other Wireless Applications," *IEEE Antennas Wirel. Propag. Lett.*, vol. 11, pp. 539–542, 2012.

[5] J. Pei, A. G. Wang, S. Gao, and W. Leng, "Miniaturized Triple-Band Antenna with a Defected Ground Plane for WLAN/WiMAX Applications," *IEEE Antennas Wirel. Propag. Lett.*, vol. 10, pp. 298–301, 2011.

[6] L. Li, X. Zhang, X. Yin, and L. Zhou, "Compact Triple-Band Printed Monopole Antenna for WLAN/WiMAX Applications," *IEEE Antennas Wirel. Propag. Lett.*, vol. 15, pp. 1853–1855, 2016.

[7] D. H. Werner and S. Ganguly, "An overview of fractal antenna engineering research," *IEEE Antennas Propag. Mag.*, vol. 45, no. 1, pp. 38–57, Feb. 2003.

[8] J. P. Gianvittorio and Y. R. Samii, "Fractal antennas: A novel antenna miniaturization technique and applications," *IEEE Antennas Propag. Mag.*, vol. 44, no. 1, pp. 20–36, Feb. 2002.

[9] C. Borja and J. Romeu, "On the behavior of Koch island fractal boundary microstrip patch antenna'," *IEEE Trans. Antennas Propag.*, vol. 51, no. 6, pp. 1281–1291, Jun. 2003.

[10] K. C. Hwang, "A Modified Sierpinski Fractal Antenna for Multiband Application," *IEEE Antennas Wirel. Propag. Lett.*, vol. 6, pp. 357–360, 2007.

[11] D. D. Krishna, M. Gopikrishna, C. K. Anandan, P. Mohanan, and K. Vasudevan, "CPW-Fed Koch Fractal Slot Antenna for WLAN/WiMAX Applications," *IEEE Antennas Wirel. Propag. Lett.*, vol. 7, 2008.

[12] D. D. Krishna, M. Gopikrishna, C. K. Aanandan, P. Mohanan, and K. Vasudevan, "Compact Wide Band Koch Fractal Printed Slot Antenna," *IET Microw. Antennas Propag.*, vol. 3, no. 5, pp. 782–789, 2009.

[13] S. N. Sinha and M. Jain, "A self-affine fractal multiband antenna," *IEEE Antennas Wirel. Propag. Lett.*, vol. 6, pp. 110–112, 2007.

[14] B. Manimegalai, S. Raju, and V. Abhaikumar, "A Multifractal Cantor Antenna for Multiband Wireless Applications," *IEEE Antennas Wirel. Propag. Lett.*, vol. 8, pp. 359–362, 2009.

[15] N. Bayatmaku, P. Lotfi, M. Azarmanesh, and S. Soltani, "Design of Simple Multiband Patch Antenna for Mobile Communication Application Using New E-Shape Fractal," *IEEE Antennas Wirel. Propag. Lett.*, vol. 10, 2011.

[16] A. Aggarwal and M. V. Kartikeyan, "Pythagoras tree: A fractal patch antenna for multifrequency and ultra wide bandwidth operation," *Prog. Electromagnet. Res. C*, vol. 16, pp. 25–35, 2010.

[17] W. C. Weng and C. L. Hung, "An H-Fractal antenna for multiband applications," *IEEE Antennas Wirel. Propag. Lett.*, vol. 13, pp. 1705–1708, 2014.

[18] A. Gupta, H. Dutt, and R. Khanna, "An X-shaped fractal antenna with DGS for multiband applications," *Int. J. Microwave Wirel. Technol.*, vol. 9, no. 5, pp. 1075–1083, 2016.

[19] J. Pourahmadazar, C. Ghobadi, J. Nourinia, and H. Shirzad, "Multiband ring fractal monopole antenna for mobile devices," *IEEE Antennas Wirel. Propag. Lett.*, vol. 9, pp. 863–866, 2010.

[20] P. Beigi, J. Nourinia, Y. Zehforoosh, and B. Mohammadi, "A compact novel CPW-fed antenna with square spiral patch for multiband applications," *Microwave Opt. Technol. Lett.*, vol. 57, no. 1, pp. 111–115, Jan. 2015.

[21] P. Beigi and P. Mohammadi, "A novel small triple-band monopole antenna with crinkle fractal-structure," *Int J Electron. Commun. (AEÜ)*, vol. 70, no. 10, pp. 1392–87, 2016.